Nonreciprocal waveguide Bragg gratings

Mykola Kulishov [a, b], Jacques M. Laniel [a], Nicolas Bélanger [a], José Azaña [c], David V. Plant [a]

[a] *Department of Electrical and Computer Engineering, Photonic System Group, McGill University, Montreal (Quebec) H3A 2A7, Canada*
jlaniel@ photonics.ece.mcgill.ca , nbelan@ photonics.ece.mcgill.ca , plant@photonics.ece.mcgill.ca
[b] *Adtek Photomask Inc., 4950 Fisher str., Montreal (Quebec) H4T 1J6, Canada*
mkulishov@adetkphotomask.com
Institut National de la Recherche Scientifique - Énergie, Matériaux et Télécommunications (INRS-EMT), 800 de la Gauchetière Ouest, suite 6900. Montréal (Québec) H5A 1K6 Canada
azana@emt.inrs.ca

Abstract: The use of a complex short-period (Bragg) grating which combines matched periodic modulations of refractive index and loss/gain allows asymmetrical mode coupling within a contra-directional waveguide coupler. Such a complex Bragg grating exhibits a different behavior (e.g. in terms of the reflection and transmission spectra) when probed from opposite ends. More specifically, the grating has a single reflection peak when used from one end, but it is transparent (zero reflection) when used from the opposite end. In this paper, we conduct a systematic analytical and numerical analysis of this new class of Bragg gratings. The spectral performance of these, so-called nonreciprocal gratings, is first investigated in detail and the influence of device parameters on the transmission spectra of these devices is also analyzed. Our studies reveal that in addition to the nonreciprocal behavior, a nonreciprocal Bragg grating exhibits a strong amplification at the resonance wavelength (even with zero net-gain level in the waveguide) while simultaneously providing higher wavelength selectivity than the equivalent index Bragg grating. However, it is also shown that in order to achieve non-reciprocity in the device, a very careful adjustment of the parameters corresponding to the index and gain/loss gratings is required.

OCIS codes: (230.3120) Integrated optics devices; (230.1950) Diffraction gratings, (250.4480) Optical amplifiers

References and links

1. X. Daxhelet, M. Kulishov, "Theory and practice of long-period gratings: when a loss becomes a gain," Opt. Lett. **28**, 686-688 (2003).
2. M. Kulishov, V. Grubsky, J. Schwartz, X. Daxhelet, D.V. Plant, "Tunable waveguide transmission gratings based on active gain control," IEEE J. Quantum Electron. **40**, 1715-1724 (2004).
3. L. Poladian, "Rresonance mode expansions and exact solutions for nonuniform gratings," Physical Review E **54**, 2963-2975 (1996).
4. M. Greenberg, M. Orenstein, "Irreversible coupling by use of dissipative optics," Opt. Lett. **29**, 451-453 (2004).
5. M. Greenberg, M. Orenstein, "Unidirectional complex gratings assisted couplers," Opt. Express **12**, 4013-4018 (2004), http://www.opticsexpress.org/abstract.cfm?URI=OPEX-12-17-4013.
6. R. Kashyap, *Fiber Bragg Gratings* (SanDiego, CA: Academic, 1999, ch.4).
7. T. Erdogan, "Fiber grating spectra," J. Lightwave Technol. **15,** 1277-1294 (1997).
8. H. Kogelnik, C.V. Shank, "Coupled mode theory of distributed feedback lasers," J.Appl.Phys. **43**, 2327-2335 (1972).
9. D.R. Zimmerman, L.H. Spiekman, "Amplifiers for the masses: EDFA, EDWA, and SOA Amplets for metro and access applications," IEEE J. Lightwave Technol. **22**, 63-71 (2004).

#6649 - $15.00 US Received 22 February 2005; revised 6 April 2005; accepted 6 April 2005

1. Introduction

While losses in integrated optics devices are generally detrimental, it has been also shown that properly tailored optical losses can be exploited, allowing even the creation of new device functionalities [1]. For instance, it has been recently demonstrated that in long-period grating (LPG) – based devices, new and interesting wavelength filtering operations (e.g. tunable wavelength filters) can be implemented by properly controlling the cladding – mode losses [2]. Furthermore, the gain/loss coefficient, or imaginary part of the refractive index, can be controlled through the injected carrier concentration in semiconductor waveguides or by changing the pumping conditions in rare-earth-doped fibers.

In an earlier work [3], Poladian showed theoretically that if the imaginary component of the refractive index in a Bragg grating is also periodically modulated, then the conventional symmetry in the contra-propagating mode interaction in these devices can be "broken". This leads to an asymmetrical behavior in this mode coupling process; specifically the Bragg grating will induce coupling from the forward-propagating mode into the backward-propagating mode when the light is launched from one end of the grating but the same is not true when the light is launched from the opposite end. Poladian suggested that the grating profile required to exhibit ideal asymmetric operation might be achieved by using a perfectly matched combination of index and gain/loss gratings [3]. In this paper we will use the term "nonreciprocal" Bragg grating (NBG) to refer to this new class of complex gratings. However, it should be noted that the term "nonreciprocal" in the present context has a different meaning to that in the context of the Lorentz reciprocity theorem. In fact, it should be emphasized that optical-isolating devices cannot be created on the basis of the NRBGs studied here, unless additional magneto-optic or nonlinear effects are included.

In conventional index Bragg gratings (IBGs) with a periodic modulation of the real refractive index, the symmetry in two-mode coupling is associated with the symmetry of the Fourier transform of any real function (e. g. a sine or cosine function). Nonreciprocal mode interaction is achieved when the periodic perturbation is described by a purely imaginary function that has only single-sided spatial components: $\Delta\tilde{n} = \Delta n_o \exp(j2\pi z/\Lambda)$. This perturbation can be practically realized using a combination of an index grating (real grating) and a gain/loss grating (imaginary grating) of the form $\exp(\pm j2\pi z/\Lambda) = \cos(2\pi z/\Lambda) \pm j\sin(2\pi z/\Lambda)$. Since the original suggestion by Poladian [3], to the best of our knowledge, there has been no systematic study of NRBGs, as well as no investigation on how deviations from the predicted ideal distribution of the complex perturbation can affect the grating device performance. More recently, Greenberg and Orenstein [4] have stated that a complex grating of the form $\exp(\pm j2\pi z/\Lambda)$ can also be used "to break the space-time reversibility in (two) co-propagating mode interaction within a grating-assisted co-directional coupler". This original work has been followed by another more detailed study on the same topic [5]. These recent works have focused on the case of co-directional coupling and again, no detailed analysis on the counterpart effect in contra-directional (Bragg) couplers has been provided.

The objective of this paper is to analyze in detail the spectral performance and design constraints of the NRBGs. The spectral features of ideal NRBGs are first studied, emphasizing some unique aspects of the spectral behavior of these gratings with a potential interest in practical applications. The robustness of this concept is then evaluated by investigating how deviations from the ideal complex grating distribution (e.g., mismatching in the amplitudes of the perturbations or spatial locations of the two gratings) affect the device spectral characteristics.

2. Theoretical model of NRBG

The modeling of the NRBGs is based on coupled mode theory [6]. The NRBG is defined as a periodic longitudinal perturbation of the complex refractive index, which includes both the index (real) grating and the gain/loss (imaginary) grating (the period of the perturbation is assumed to be the same for the two gratings, i.e., Λ). This perturbation can be expressed as follows:

#6649 - $15.00 US Received 22 February 2005; revised 6 April 2005; accepted 6 April 2005

$$\Delta n = \Delta n_{DC} + j\frac{\Delta\alpha_{DC}}{k_0} + \Delta n_{AC}\cos\left[\frac{2\pi}{\Lambda}z\right] - j\frac{\Delta\alpha_{AC}}{k_0}\sin\left[\frac{2\pi}{\Lambda}(z+\Delta z)\right], \quad (1)$$

where Δn_{DC} and Δn_{AC} are respectively the constant and modulated perturbation to the refractive index and $\Delta\alpha_{DC}$ and $\Delta\alpha_{AC}$ are respectively the constant and modulated perturbation to the loss/gain, and $k_0 = 2\pi/\lambda$ where λ is the wavelength in vacuum. Eq. (1) is a general description of a complex grating and it takes into account the following: the DC and AC terms can have different amplitudes; the real and imaginary gratings can also exhibit different amplitudes; and the phase difference between the two gratings is not necessarily $\pi/2$. Specifically, the term Δz represents the additional phase shift between the cosine (real) and the sine (imaginary) gratings. Notice that Eq. (1) does not include the effect of gain or loss saturation. It is important to emphasize that ideal non-reciprocal behavior is achieved when (i) the phase difference between the index and gain/loss gratings is exactly $\pi/2$ ($\Delta z = 0$) and (ii) both gratings exhibit an identical strength ($\Delta n_{AC} = \Delta\alpha_{AC}/k_0$). In this case, the refractive index perturbation is described by a purely imaginary function that has only single-sided spatial components. As mentioned in the introduction, this is the fundamental requirement to ensure a non-reciprocal behavior in the grating structure.

Here we consider a Bragg grating within a single-mode waveguide. It is assumed that the waveguide is weakly guiding and no energy is coupled to radiation modes [6]. The propagation constant of the fundamental propagating mode is β. The perturbation given by Eq. (1) will induce power transference from the forward-propagating mode ($+\beta$) into the backward-propagating mode ($-\beta$) at the phase-matching wavelength. The evolution of the forward-propagating, $A(z)$, and backward-propagating, $B(z)$, mode amplitudes within the slowly varying envelope approximation is determined by the following equations [6, 7]:

$$\frac{dA}{dz} = j\tilde{\sigma}A + j\kappa_{12}B\exp\left[-j2\Delta\beta z\right], \quad (2)$$

$$\frac{dB}{dz} = -j\tilde{\sigma}B - j\kappa_{21}A\exp\left[j2\Delta\beta z\right], \quad (3)$$

where $\tilde{\sigma} = \sigma + j\alpha$, and σ and α are proportional to the non-modulated real and imaginary part of Eq. (1), $\Delta\beta = \beta - \pi/\Lambda$ and the coupling coefficients are:

$$\kappa_{12} = \left[\kappa_n - \kappa_\alpha\exp\left(j2\pi\Delta z/\Lambda\right)\right], \quad (4)$$

$$\kappa_{21} = \left[\kappa_n + \kappa_\alpha\exp\left(-j2\pi\Delta z/\Lambda\right)\right]. \quad (5)$$

The coupling coefficients κ_n and κ_α are proportional to the overlap between the spatial mode distributions of each waveguide and the AC component of Eq.(1). It is important to point out that α represents the gain/loss coefficient experienced by the propagating fields. Therefore, the gain/loss associated with the intensities is given by 2α. The gain or loss experienced by the propagating modes can be modeled by either taking $\alpha_i > 0$ for loss or $\alpha_i < 0$ for gain. In order to simplify Eqs. (2) and (3), it is possible to define a complex propagation constant $\tilde{\beta} = \beta + \sigma + j\alpha$ and a complex phase-matching factor: $\hat{\sigma} = \tilde{\beta} - \pi/\Lambda$. Eq. (2) and (3) can then be re-written as follows:

$$\frac{dR}{dz} = j\hat{\sigma}R + j\kappa_{12}S, \quad (6)$$

$$\frac{dS}{dz} = -j\hat{\sigma}S - j\kappa_{21}R, \quad (7)$$

where new mode amplitudes are defined as:

#6649 - $15.00 US Received 22 February 2005; revised 6 April 2005; accepted 6 April 2005

$$R(z) = A(z)\exp[j\Delta\beta z] \tag{8}$$

$$S(z) = B(z)\exp[-j\Delta\beta z] \tag{9}$$

In the ideal case when there is no shift between the index and gain gratings ($\Delta z = 0$), the coupling coefficients are:

$$\kappa_{12} = (\kappa_n - \kappa_\alpha), \tag{10}$$

$$\kappa_{21} = (\kappa_n + \kappa_\alpha). \tag{11}$$

Eqs. (10) and (11) show that when the modulation of the real grating is equal to the modulation of the imaginary grating, the coupling coefficient κ_{12} is cancelled out, i.e., $\kappa_n - \kappa_\alpha = 0$.

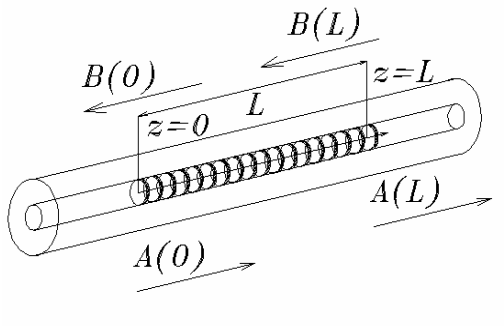

Fig. 1. Schematic for the interacting modes, *A(z)* and *B(z)*, in the Bragg grating.

Figure 1 shows the structure of the Bragg grating and the interacting modes. The ends of the grating are located at $z = 0$ and L. The solutions for the coupling equations (6) and (7) are obtained by using 2x2 transfer matrices **M** [7]. The matrix describing the transmission through the uniform complex grating relates the complex amplitudes $A(L)$ and $B(L)$ with the complex amplitudes $A(0)$ and $B(0)$ in the following way:

$$\begin{bmatrix} A(L) \\ B(L) \end{bmatrix} = \begin{bmatrix} M_{11} & M_{12} \\ M_{21} & M_{22} \end{bmatrix} \begin{bmatrix} A(0) \\ B(0) \end{bmatrix}, \tag{12}$$

and has the following elements:

$$\begin{aligned}
M_{11} &= \left[\cosh(\gamma L) + j\frac{\hat{\sigma}}{\gamma}\sinh(\gamma L)\right]\exp\left[-j\left(\hat{\sigma} - \tilde{\beta}\right)L\right], \\
M_{12} &= j\frac{\kappa_{12}}{\gamma}\sinh(\gamma L)\exp\left[-j\left(\hat{\sigma} - \tilde{\beta}\right)L\right], \\
M_{21} &= -j\frac{\kappa_{21}}{\gamma}\sinh(\gamma L)\exp\left[j\left(\hat{\sigma} - \tilde{\beta}\right)L\right], \\
M_{22} &= \left[\cosh(\gamma L) - j\frac{\hat{\sigma}}{\gamma}\sinh(\gamma L)\right]\exp\left[j\left(\hat{\sigma} - \tilde{\beta}\right)L\right],
\end{aligned} \tag{13}$$

where $\gamma = \left(\kappa_{12}\kappa_{21} - \hat{\sigma}^2\right)^{1/2}$. It is important to point out that the matrix elements given by Eq. (13) contain complex parameters. The only real parameter in (13) is the position z along the grating. If a signal is injected from the left side of the grating, $A(0) = 1$ and therefore $B(L) = 0$, (see Fig. 1) then the complex amplitude of the reflected signal is given by $B(0) = -M_{21}/M_{22}$ and the complex amplitude of the transmitted signal is given by $A(L) = M_{11} - M_{12}M_{21}/M_{22}$. On the other hand, if the signal is launched from the right side of the grating, i.e. $B(L) = 1$ and

#6649 - $15.00 US Received 22 February 2005; revised 6 April 2005; accepted 6 April 2005

therefore $A(0) = 0$, then the complex amplitude of the reflected signal is given by $A(L) = M_{12}/M_{22}$ and the complex amplitude of the transmitted signal is given by $B(0) = 1/M_{22}$.

3. Spectral and dispersion characteristics of NRBGs

In the numerical simulations presented here, the following effective index for the reflected mode is $n_{eff} = 1.55$ (the propagation constant is then given by $\beta = k_0 n_{eff}$). It is assumed here that the effective index is equal to the group index of the propagation mode. The grating period which allows coupling between the forward- and backward-propagating modes at a resonant wavelength of 1550 nm is $\Lambda = 0.5$ μm. In all the cases, the spectra are calculated assuming a grating of length $L = 5$ mm.

Figure 2 presents reflection (red, solid) and transmission (blue, dash) spectra for Fig. 2(a) IBG ($\kappa_n L = \pi/2$, $\kappa_\alpha = 0$) and Fig. 2(b) ideal NRBG ($\kappa_n = \kappa_\alpha$, $\Delta z = 0$) for $\kappa_{21} L = (\kappa_\alpha + \kappa_n) L = \pi$. It is important to point out that in our calculations, we neglect any contributions from the DC component in Eq. (1), which means that we assume that $\sigma = 0$ and $\alpha = 0$.

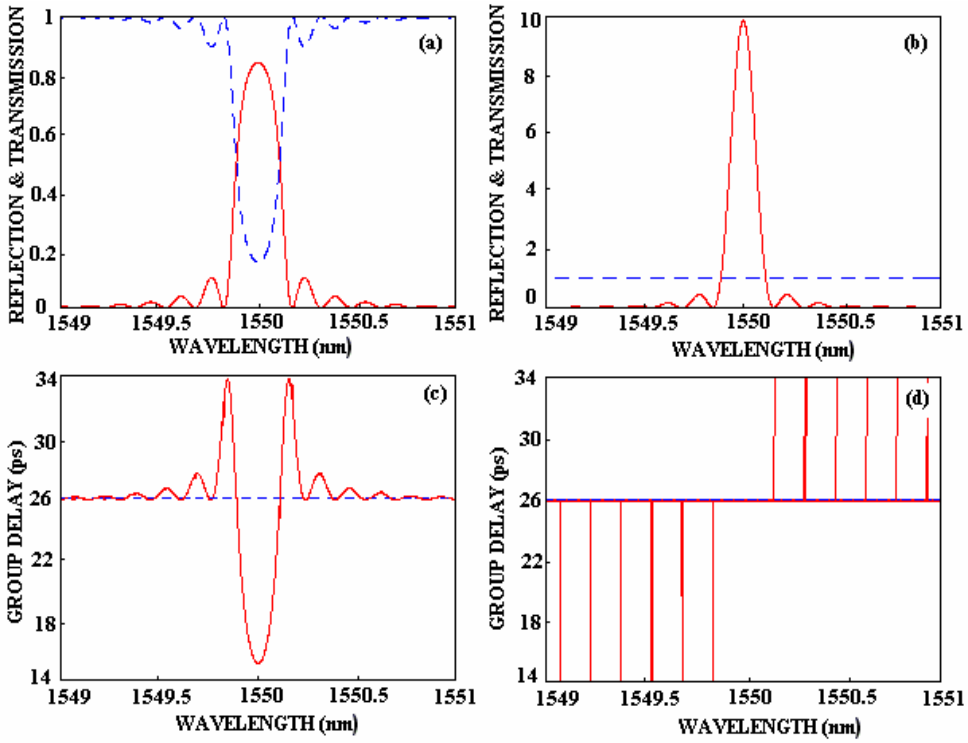

Fig. 2. Transmission (blue, dash) and reflection (red, solid) spectra of a IBG ($\kappa_n L = \pi/2$, $\kappa_\alpha = 0$) (a) and an ideal NRBG ($\Delta z = 0$ and $\kappa_n = \kappa_\alpha$, so that $\kappa_{21} L = (\kappa_\alpha + \kappa_n) L = \pi$) (b). The group delay (red, solid) of the reflected light is shown in (c) and (d) with respect to (a) and (b) respectively. The length of the grating is 5 mm.

The transfer matrix for the *ideal* NRBG takes the following form:

$$M = \begin{bmatrix} \exp\left(j\tilde{\beta}L\right) & 0 \\ -j\frac{\kappa_{21}}{\hat{\sigma}}\sin(\hat{\sigma}L)\exp\left[j\left(\hat{\sigma}-\tilde{\beta}\right)L\right] & \exp\left(-j\tilde{\beta}L\right) \end{bmatrix} \qquad (14)$$

If the light is launched at $z = 0$ so that the boundary condition are $A(0) = 1$ and $B(L) = 0$ (see Fig.1), we can infer from Eq. (12) that the transmitted light is $A(L) = M_{11} = \exp(j\tilde{\beta}L)$ and the reflected light is $B(0) = -M_{21}/M_{22}$ (which is the case showed in Fig. 1(b). However, if the optical signal is injected into the right end of the grating, $B(L) = 1$ and $A(0) = 0$, then there is

#6649 - $15.00 US
Received 22 February 2005; revised 6 April 2005; accepted 6 April 2005

complete light transmission: $B(0) = 1/M_{22} = \exp(j\tilde{\beta}L)$ with zero reflection $A(L) = 0$. In other words, as expected, the mode coupling process is strongly asymmetric in this structure.

A significant difference between an IBG and a NRBG is that the latter allows one to add a signal through reflection without simultaneously dropping the transmitted signal (as for the case of regular gratings). This can be observed in Fig. 2(b). Furthermore, it is worth noting that the reflected signal is wavelength dependent, while the transmitted signal remains constant in wavelength. Indeed, as it can be inferred from the transfer matrix Eq. (14), light propagates through the grating as if there were no grating in the waveguide.

3.1 Amplification mechanism

As we can see from Fig. 2(a), the IBG with $\kappa_n L = \pi/2$ is only moderately strong, i.e. it provides a reflectivity slightly higher than 80% at the resonance wavelength. However, combination of this weak index grating with the complementary grating of gain/loss (of the same strength $\kappa_\alpha L = \pi/2$) results in surprisingly strong reflection combined with amplification of almost 10 dB. It is important to point out that the spectra shown in Fig. 2 were computed for zero DC amplification in the waveguide ($\alpha = 0$). Equal segments of gain and loss in the imaginary grating imply no net gain or loss along the grating. However, the power conservation law is not violated here since the complex grating is an active structure and power is supplied to maintain optical gain.

The mechanism of the strong amplification becomes evident from a simple analysis of the electric field inside the NRBG. For the ideal NRBG ($\kappa_n = \kappa$ and $\kappa_\alpha = \kappa$), its imaginary counterpart is defined by the following equation:

$$\Delta n(z) = -j\frac{\Delta\alpha_{AC}}{k_0}\sin[2\pi z/\Lambda] \tag{15}$$

We know that for when Im{Δn} of Eq. (15) is positive, it represents loss while when it is negative, it represents gain. At the phase matching condition ($\Delta\beta = 0$) and no DC contribution, Eqs. (2) and (3) are greatly simplified, and for $A(0) = A_0$ and $B(L) = 0$, these equations have the following solutions: $A(z) = A_0$ and $B(z) = -2j\kappa A_0(z - L)$. The electric field distribution inside the NRBG is then given by the following relation:

$$E(z) = E^+(z) + E^-(z) = \frac{1}{2}\left[A(z)\exp(+j\pi z/\Lambda) + B(z)\exp(-j\pi z/\Lambda)\right] + c.c. \tag{16}$$

where $E^+(z)$ and $E^-(z)$ are respectively the forward and backward propagating fields inside the device. As a result, the field intensity inside the NRBG, $E(z)E^*(z)$, is found to be

$$I(z) = |A_0|^2\left[1 + 4\kappa^2(z-L)^2 - 4\kappa(z-L)\sin(2\pi z/\Lambda)\right] \tag{17}$$

As we can see from equation (17), the field intensity modulation is always in phase with the gain grating and this condition is satisfied for any values of κL. Figure 3 shows the field intensity inside the grating with respect to the gain grating periodicity.

It is evident that a constructive interaction between the forward- and backward-propagating modes in the gain segments of the imaginary grating is responsible for amplification of the reflected wave. At the same time, the asymmetric distribution of the complex perturbation prevents the mode interaction when the signal is launched from the opposite side of the grating. In this direction the NRBG ideally transmits the light without any reflection.

#6649 - $15.00 US Received 22 February 2005; revised 6 April 2005; accepted 6 April 2005

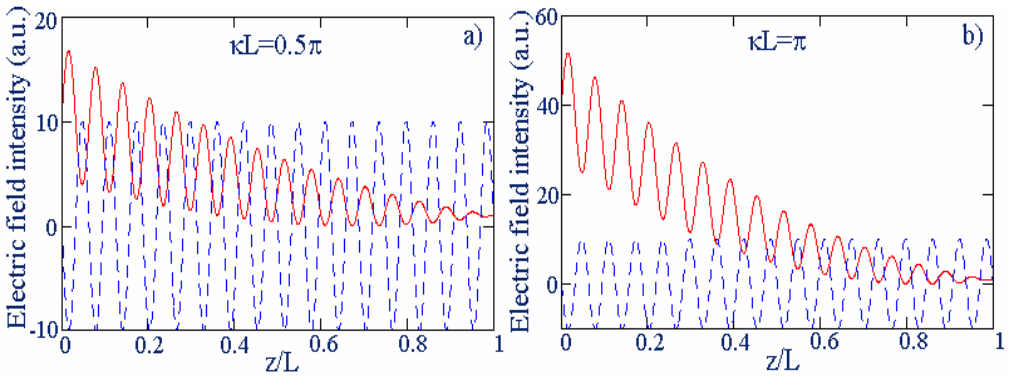

Fig. 3. Electric field intensity distribution (red, solid) inside the NRBG with respect to the imaginary grating (blue, dash) for (a) $\kappa L=\pi/2$ and (b) $\kappa L=\pi$. The negative segments of the imaginary grating correspond to the gain periods, whereas the positive ones correspond to the loss periods.

3.2 Frequency selectivity

It is also interesting to compare the reflection bandwidth of a NRBG and an IBG with the same index grating strength (e.g., $\kappa_n L = \pi$). In the NRBG, equal contributions from the real and imaginary parts result in a total grating strength of $\kappa_{21}L = \kappa_n L + \kappa_\alpha L = 2\kappa_n L = 2\pi$ (here $\kappa_{12}L = 0$). The corresponding bandwidths are estimated as the difference between the wavelength at peak reflectivity and the first zero at either side around this peak reflectivity. The respective bandwidths $\Delta\lambda_{nr}$ (for the NRBG) and $\Delta\lambda_c$ (for the IBG) are given by the following expressions:

$$\frac{\Delta\lambda_{nr}}{\lambda} = \frac{\lambda}{n_{eff} L}, \tag{18}$$

$$\frac{\Delta\lambda_c}{\lambda} = \frac{\kappa\lambda}{\pi n_{eff}} \sqrt{1+\left(\frac{\pi}{\kappa L}\right)^2}, \tag{19}$$

where $\kappa = \kappa_n$ (κ_α is zero for the conventional case). From Eqs. (18) and (19) it can be easily inferred that the bandwidth of the NRBG is always narrower than that of the IBG (this is in good agreement with our observations in Fig. 2 and Fig. 3). In other words, the NRBG offers the advantage of higher spectral selectivity as compared with a IBG. In the case of a "weak grating" limit, i.e. when $\kappa L << \pi$, the bandwidth of a IBG is described by the same equation as that of the equivalent NRBG (in this case, Eq. (19) can be approximated by Eq. (18)). However, even in this situation, the IBG has a FWHM bandwidth twice broader than the NRBG with the same index modulation strength (this is actually related to the fact that $\kappa_{21} = 2\kappa_n$). The "weak grating" limit corresponds with the case when light penetrates the full length of the IBG (in a NRBG, the light penetrates the full grating length, regardless the perturbation strength). We recall that for an IBG in the "strong grating" limit, $\kappa L >> \pi$, all the light is reflected along a short section at the input end of the grating, and thus the bandwidth is independent of length and directly proportional to the coupling coefficient. Further, as Fig. 2(b) shows, the transmission of an ideal NRBG is completely insensitive to the grating strength κL while its reflection is proportional to the grating strength (when neglecting gain saturation).

3.3 Dispersion Characteristics of NRBGs

An additional feature of the NRBG is that as shown in Fig. 2(d), it is completely dispersionless; for comparison, we recall that the same is not true for a IBG, where the dispersion in the reflected band is not null but rather significant towards the edges of this band (see Fig. 2(c)). In contrast, a NRBG with negligible average (net) gain/loss does not introduce

#6649 - $15.00 US Received 22 February 2005; revised 6 April 2005; accepted 6 April 2005

any dispersion at all the wavelengths. In Fig. 2(d), the group delay is constant as a function of wavelength and its value corresponds to the time required for the mode to propagate through the grating, $n_{eff}L/c$, where c is the speed of light in vacuum. This time is also marked by the blue dotted line in Fig. 2(c). At wavelengths of zero reflection, the phase undergoes discontinuities, which translate into the observed sharp jumps (delta functions) in the group delay characteristic.

When a net gain/loss is introduced in the guide(s), a wavelength-dependant group delay is observed, and in particular, the discontinuities at the zero reflection wavelengths, gradually spread into bandwidth limited peaks.

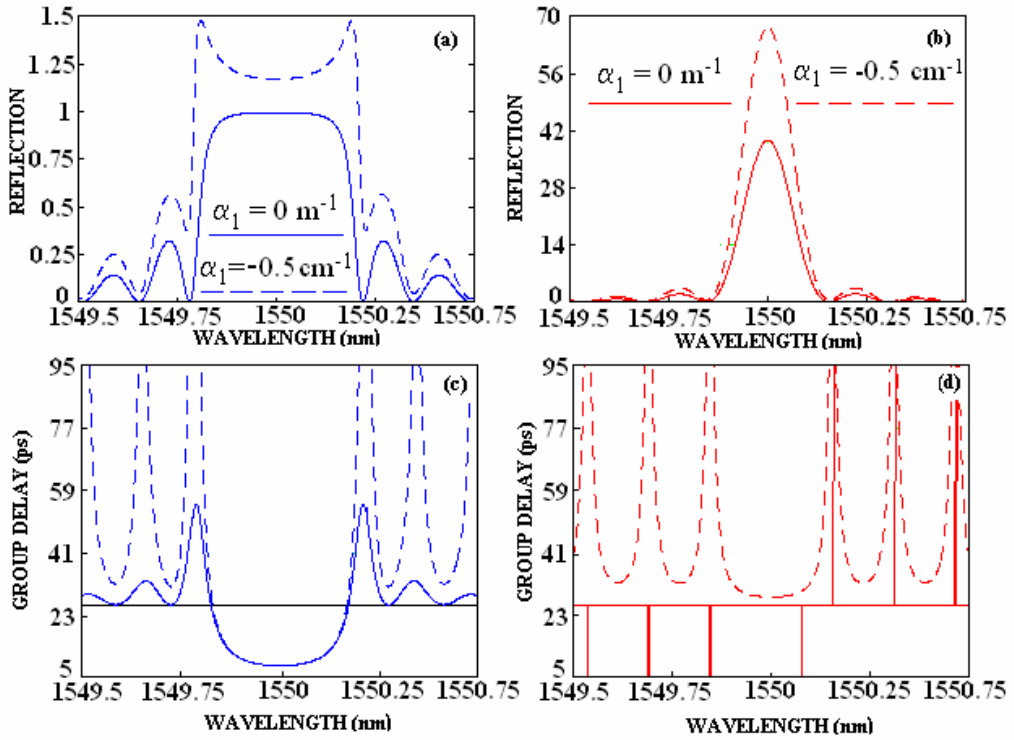

Fig. 4. (a) Reflectivity and (c) the group delay of the IBG (blue, $\kappa_n L = \pi$; $\kappa_\alpha = 0$) and (b) reflectivity and (d) group delay of the ideal NRBG (red, $\Delta z = 0$, $\kappa_{21}L = (\kappa_\alpha + \kappa_n)L = 2\pi$, $\kappa_{12} = 0$) for the gratings with zero net gain (solid, $\alpha = 0$) and nonzero net gain (dash, α = - 0.5 cm^{-1} in the waveguide). All the gratings are assumed to be 5mm long.

3.4 Effect of net gain in the waveguide

Another remarkable behavior of the nonreciprocal grating is demonstrated in Fig. 4, where we introduce a non-zero net gain into the waveguide (through imaginary part of the propagation constant, α). As it can be seen in Fig. 4(a), when α becomes negative (which means that a pump is applied providing a net gain) two symmetrical maxima near the edges of the IBG reflection band arise. These maxima grow as the net gain increases. This phenomenon is called threshold degeneracy and was first described for distributed feedback (DFB) lasers [8]. In contrast, the reflection spectra corresponding to the NRBG in Fig. 4(b) shows a single peak of amplification at the resonance wavelength. Moreover, this amplification is much more efficient than that of the IBG (blue, dash). One can also notice that in general, the dispersion characteristics are strongly affected by the presence of net gain in the guide, and this distortion within the reflection bandwidth is especially significant in the case of NRBG (Fig. 4(d)). These observations lead us to the conclusion that in the case of a NRBG, amplification

#6649 - $15.00 US Received 22 February 2005; revised 6 April 2005; accepted 6 April 2005

can be better controlled by the grating strength, rather than by introducing a higher net grain (e.g., by increasing the pump power).

Finally, to give a reference, a typical maximum index modulation of 10^{-4} corresponds to a gain peak of approximately $2\alpha = 4.05$ cm^{-1} (35 dB/cm) (for a perfect matching gain grating, operating at 1550 nm). This gain level can be achieved relatively easily with current integrated technologies using semiconductor gain media [9]. This gain level is also close to be feasible in erbium-doped waveguide amplifiers (EDWA) [9] where several dB/cm gain coefficients are possible, representing a good compromise between the high erbium doping level and parasitic effects.

4. Robustness of the NRBG design

The results presented in Section 3 have been calculated for an ideal NRBG, where both real and imaginary gratings have equal amplitudes ($\kappa_n = \kappa_\alpha$), and they are shifted exactly a quarter of the period with respect to each other ($\Delta z = 0$). Our objective now is to evaluate the impact of deviations from these ideal conditions on the grating's spectral characteristics.

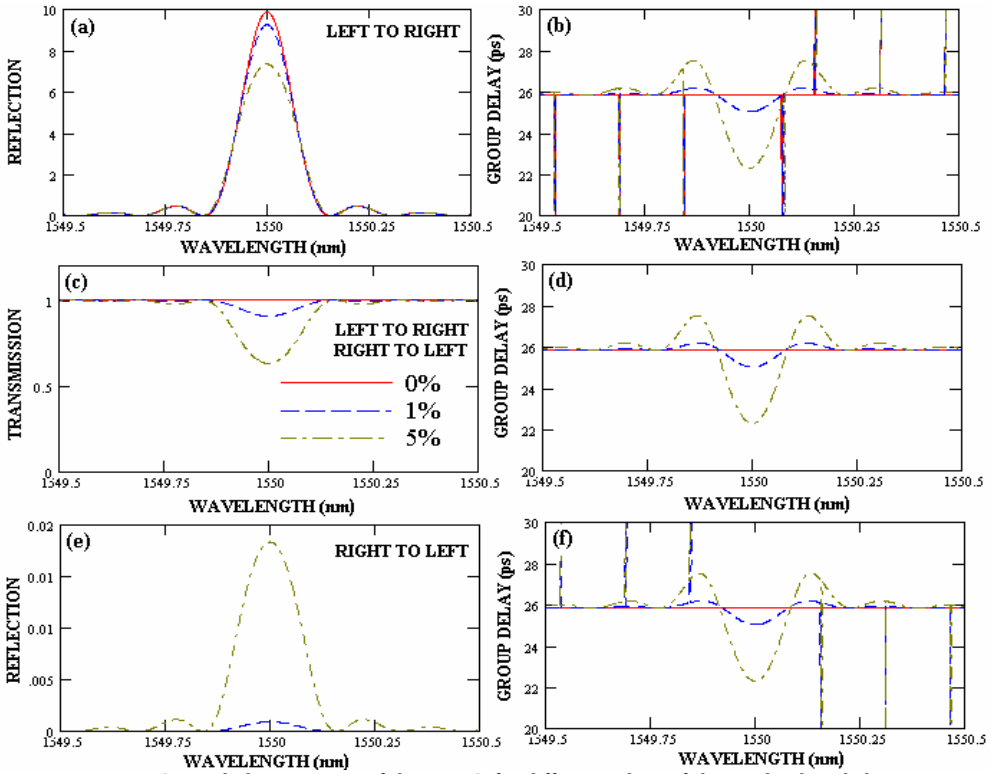

Fig. 5. Spectral characteristics of the NRBG for different values of the amplitude imbalance between the real κ_n and κ_α imaginary components. There is no grating position deviation ($\Delta z = 0$): (a) reflection spectrum and (b) reflection group delay for light launched into the left side of the grating ($z = 0$); (c) transmission spectrum and (d) transmission group delay (the transmission characteristics are the same regardless the light input direction, $z = 0$ or L); (e) reflection spectrum and (f) reflection group delay for light injected into the right side of the grating ($z = L$).

4.1 Grating amplitude misbalance

As shown in Fig. 5, imbalance between the real and imaginary amplitudes of the NRBG, κ_n and κ_α, affects the transmission spectra (as compared with those of the ideal NRBG). It is important to point out that in our simulations, we assume perfect phase matching between the

#6649 - $15.00 US Received 22 February 2005; revised 6 April 2005; accepted 6 April 2005

index and the gain gratings, i.e. $\Delta z = 0$. In all the plots in Fig. 5, the solid (red) curves correspond to the case of an ideal grating or 0% difference between the respective amplitudes (the difference is given by $2(\kappa_n-\kappa_\alpha)/(\kappa_n+\kappa_\alpha)$) in the grating amplitudes), the dashed (blue) curves correspond to a 1% difference, and the dash-dotted (brown) curves correspond to a 5% difference. As we can see, the grating amplitude imbalance of 5% leads to i) small reduction of amplified reflection (~ 1.2 dB) for the wave incident from the left side (Fig. 5a); ii) approximately 2 dB deviation from perfect 100% transmission (Fig. 5(c)); iii) and slight increase in reflection from right to left from zero to –18 dB (Fig. 5(e)). If one neglects sharp peaks on the plots for the group delay (Fig. 5(b), Fig. 5(d), Fig. 5(f)), the reflected and both transmitted waves exhibit practically the same deviation from the ideal non-dispersive behavior.

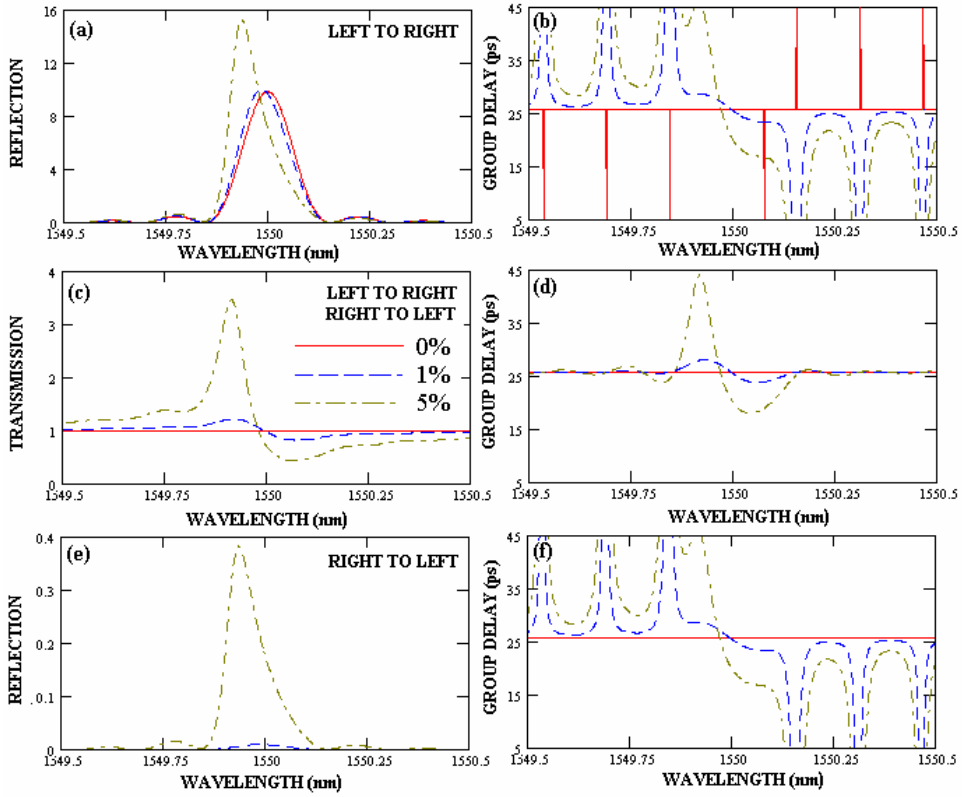

Fig. 6. Spectral characteristics of the NRBG for the different values of the grating position deviation Δz between the real and imaginary gratings. There is no grating amplitude imbalance ($\kappa_n = \kappa_\alpha$). (a) reflection spectrum and (b) reflection group delay for light launched into the left side of the grating ($z = 0$); (c) transmission spectrum and (d) transmission group delay (transmission characteristics are the same regardless the light input direction $z = 0$ or L); (e) reflection spectrum and (f) reflection group delay for light injected into the right side of the grating ($z = L$).

4.2 Grating position deviation

The next potential imbalance between the index and gain gratings may be induced by deviation, Δz, from the ideal position of real and imaginary gratings (ideally $\Delta z = 0$). Fig. 6 presents simulations for amplitude-matching gratings ($\kappa_n = \kappa_\alpha$) with different values of position imbalance: $\Delta z/\Lambda = 0\%$ (solid, red), $\Delta z/\Lambda = 1\%$ (dash, blue) and $\Delta z/\Lambda = 5\%$ (dot, magenta). Unlike the amplitude imbalance, the 5% position deviation leads to i) the shift in the resonance wavelength of the reflected light in Fig. 6(a) accompanied by ~ 2 dB increase in

#6649 - $15.00 US
Received 22 February 2005; revised 6 April 2005; accepted 6 April 2005

peak amplification; ii) ~ 5 dB deviation from perfect 100% transmission (Fig. 6(c)); iii) and substantial increase in reflection from right to left from zero to –4 dB (Fig. 6(e)). The position imbalance also produces strong dispersion especially within the reflection band, as it can be seen in Fig. 6(b) and Fig. 6(f). Notice that the position deviation generally imposes a stricter tolerance on the grating design, than the amplitude imbalance.

5. Conclusion

In this paper, the coupled mode equations corresponding to a general complex Bragg grating perturbation, i.e., combination of real grating (index perturbation) and imaginary grating (gain/loss perturbation), in an optical waveguide were introduced and solved. The solution to these equations was first obtained for the case of a complex grating providing an ideal nonreciprocal behavior. Our analysis reveals unique characteristics for these complex gratings (as compared with conventional index Bragg gratings). In addition to the anticipated nonreciprocal behavior, a complex Bragg grating exhibits a strong amplification at the resonance wavelength even with zero net gain/loss level in the waveguide. This amplification occurs only within a narrow reflection wavelength band, thus leading to a simultaneous narrowband filtering process. In fact, as a filtering device, a nonreciprocal grating exhibits i) a high wavelength selectivity which exceeds (at least twice) the selectivity of the equivalent index Bragg grating; and ii) a dispersionless behavior along all the filter bandwidth. The impact of deviations in the grating profile with respect to the conditions for achieving an ideal nonreciprocal behavior has been numerically evaluated. Specifically, two potential deviations have been considered, namely mismatch between the amplitudes of the index and gain gratings and mismatch between their respective positions within the waveguide. In general, our numerical simulations show that the amplitude imbalance should be < 5% while the position deviation should be < 1% in order to ensure less than 1 dB deviation from ideal regime in transmission and less than –20 dB of reflection from the "non-reflecting" end of the grating.

Besides the intrinsic physical interest of the results presented here, they also point to nonreciprocal Bragg gratings as potentially interesting components from a more practical perspective. For instance, a device with all the combined features of a single nonreciprocal Bragg grating (dispersionless, narrowband filter incorporating amplification) may be attractive for applications in the context of DWDM optical communication systems.

Acknowledgments

This work was supported by the Natural Sciences and Engineering Research Council (NSERC) and industrial and government partners, through the Agile All-Photonic Networks (AAPN) Research Network.

#6649 - $15.00 US Received 22 February 2005; revised 6 April 2005; accepted 6 April 2005